http://ansinet.com/itj

ITJ

ISSN 1812-5638

INFORMATION TECHNOLOGY JOURNAL

ANSInet
Asian Network for Scientific Information
308 Lasani Town, Sargodha Road, Faisalabad - Pakistan

Information Technology Journal 12 (4): 749-755, 2013
ISSN 1812-5638 / DOI: 10.3923/itj.2013.749.755

A Nonsubsampled Contourlet Transform Based Medical Image Fusion Method

[1]Shen Yu, [1]Ren Enen, [1]Dang Jian-Wu, [1]Wang Guo-Hua and [2]Feng Xin
[1]School of Electronic and Information Engineering, Lanzhou Jiaotong University, Lanzhou, 730070, China
[2]School of Information Engineering, Southwest University of Science and Technology, Mianyang, 621010, China

Abstract: Based on the multiscale geometric analysis tool nonsubsampled contourlet transform (NSCT), this study proposed a novel medical image fusion method. In the high-frequency part, after the NSCT decomposition, this algorithm used the Beamlet transform to detect edge. Then it formulated the high-frequency coefficients fusion rules according to the difference of the clustering segmentation edge density. In the low-frequency part, this algorithm adopted the local area standard deviation coefficients fusion rules. After the consistency correction, this algorithm got the reconstructed image by the nonsubsampled contourlet transform (NSCT) inverse transform on the high-frequency and low-frequency coefficients. The experiment results show that this algorithm can effectively reduce the interference of the noise on the fused image, advance the fused image linear detail expressive capability and improve the amount of information.

Key words: Nonsubsampled contourlet transform, medical image fusion, beamlet transform, clustering segmentation, low-frequency subband coefficients, high-frequency subband coefficients

INTRODUCTION

For the actual clinical applications, the 3D reconstruction of mono-modal medical images (CT, MIR, PET) could not supply the doctors with enough information (Li *et al*., 2010). Medical images are the images with variety of substances. According to the uniqueness and complexity of the imaging mechanism and human tissue structure, images of different modals supply structure complementary information without covering with each other. In cranial surgery, CT supplies the best bone tissue information. The spin echo MT image supplies information that soft tissue needs. The MR subtraction image supplies information about vasculature (Rahmim and Zaidi, 2008). These are complementary information which can merge together to increase the information amount. Image fusion is the process of combining relevant information from two or more images into a single image. The resulting image will be more informative than any of the input images. The fusion of the medical images can express and display useful information to help doctor analysis and estimate the patient condition. It can greatly improve the efficiency and reliability of the clinical diagnosis. The researchers have done much work on the medical image fusion. Guanqun *et al*. (2004) firstly used wavelet analysis in medical image fusion. Ling *et al*. (2008) proposed a wavelet transform modulus maxima based fusion methods which improved the noise rejection capability. Lei *et al*. (2011) recently used the shear wave in the medical image fusion which avoided the pseudo- Gibbs phenomena in the singular points.

The multi-scale analysis based fusion methods are widely used in the medical image confusion because of the advantages of multi-resolution, anisotropic, multi-directional. One of the core problem of the multi-scale decomposition based medical image fusion method is the choice of the multi-scale decomposition tool. The wavelet transform is one of the typical multi-scale decomposition tools (Yang *et al*., 2008). But the wavelet transform could only decompose the image to three high-frequency sub-bands in horizontal, vertical and diagonal directions. It has limited directionality. To compensate for these shortages, the researchers reconstructed the wavelet basis function. They have been proposed Ridgelet transform, Curvelet theory, Contourlet theory, Nonsubsampled Contourlet Transform (NSCT) (Da Cunha *et al*., 2005) theory and Shearlet theory etc. The NSCT has been applied to image processing field because of its directional, anisotropic and translational

Corresponding Author: Shen Yu, School of Electronic and Information Engineering, Lanzhou Jiaotong University, Lanzhou, 730070, China Tel: +086-18609311366

invariance property. Zhang and Guo (2008) proved that the NSCT has obvious advantages in spectrum reservation and spatial quality when it is used in the remote sensing image. Kong *et al.* (2011) proposed an improved NSCT model by combining the nonsubsampled pyramid decomposition mechanism and the redundant lifting inseparable wavelet. The NSCT adopted nonsubsampled pyramid (NSP) in the decomposition. The NSP has weak image detail capture ability, especially for the line capture. On this basis, the author in this study introduced the Beamlet transform which was proposed by David and Xiaoming (2001). The line in the transform domain is similar to the pot in the wavelet analysis. This algorithm could supply binary representation of the line local scale, position and direction. It can easily realize precise positioning for line. And this algorithm has low complexity.

So this study combined the NSCT and Beamlet transform to detect image edge. By the good performance of Beamlet on the image line feature detection, this algorithm analyzed the target linear characteristics from images with strong noise. The detected edge information was expressed by the form of edge density. So the line feature information detected by the Beamlet was applied to the image fusion. It greatly reduced the noise interference on fused image, improved the linear detail expressive ability on fusion image and advanced the amount of information.

NSCT TRANSFORM OF IMAGE

Compared with the traditional Contourlet transform, the NSCT also has translational invariance and reduces the infection of registration error on fusion performance. Meanwhile, each subband image got by the image decomposition had the same size with the original image. It could easily find out the correspondence between the subband images and make fusion rules (Zhang and Guo, 2007).

Similar to the Contourlet transform, the NSCT also do scale decomposition and direction decomposition separately. Firstly, the Nonsubsampled Pyramid Filter Bank (NSPFB) was used to get the image multi-scale decomposition. Then the Nonsubsampled Directional Filter Bank (NSDFB) was used to do the direction decomposition on each sub-band images at different scales:

- NSPFB NSCT gets multi-scale properties by shift-invariant filtering structure. The NSPFB has the shift-invariant property. Because it has no up-sampling structure and down-sampling structure. It is composed by the decomposition filter $\{H_0(z), H_1(z)\}$, the synthesis filter $\{G_0(z), G_1(z)\}$ and satisfies Bezout identity. Its breakdown structure is shown in Fig. 1
- NSDFB NSDFB is the shift-invariant critically sampled two-dimensional filter bank structure in the Contourlet transform. It is got by removing the up and down sampling would get the NSDFB. It is very flexible. It can decompose at certain scale in random 2^l directions to satisfy the anisotropic property. The breakdown structure is shown in Fig. 2

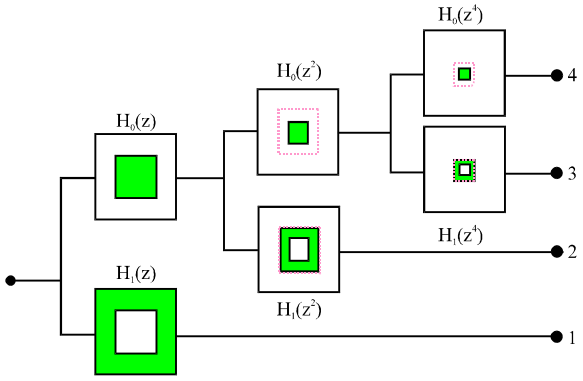

Fig. 1: The analysis part of NFPFB

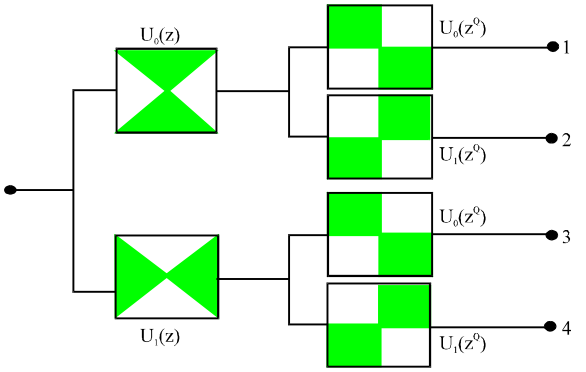

Fig. 2: The analysis part of NSDFB

The subband image was decomposed at certain scale to get 2^l directional subband coefficients. So N-level decomposition is done on the image by the NSCT to get:

$$1+\sum_{j=1}^{N} 2^{lj}$$

subband images. They are the same size with the original image.

FUSION ALGORITHM

The main steps of this algorithm are as follows:

Step 1: The low-frequency subband coefficients C^{A}_{j0} (x, y) and C^{B}_{j0} (x, y) and the high-frequency subband coefficients C_{1A} (x, y), C_{2A} (x, y), C_{3A} (x, y), C_{4A} (x, y), C_{1B} (x, y), C_{2B} (x, y), C_{3B} (x, y) and C_{4B} (x, y) was got by doing the NSCT transform on the original images A and B

Step 2: The fused low-frequency coefficient C^{F}_{j0} (x, y) was got by doing the fusion on the low-frequency subband coefficients C^{A}_{j0} (x, y) and C^{B}_{j0} (x, y). It used the local area standard deviation

Step 3: The edge images E_{1A}, E_{2A}, E_{3A}, E_{4A}, E_{1B}, E_{2B}, E_{2B}, E_{4B} were got by doing edge detection. The Beamlet transform on four high-frequency subband was used to do edge detection

Step 4: The sub_1, sub_2, sub_3, sub_4 were got by calculating marginal density function on edge image and the differences between the corresponding images

Step 5: Dual-threshold segmentation was done individually on sub_1, sub_2, sub_3, sub_4 by the Fuzzy C-Means (FCM) Clustering. Then this algorithm formulated the fusion rules of the high-frequency subband and fused the images

Step 6: This study got the fused image by regularizing the fusion results and doing NSCT inverse transform

Low-frequency subband coefficients fusion: At present, the key researches of most fusion algorithms are the high-frequency coefficients fusion rules. For the low-frequency, most algorithms adopt the simple average method. This method suppressed image noise while it also reduced the image contrast and lost the useful information in the original images. The local area standard deviation denotes the gray change intensity in this area. It also reflects the image clarity in this area to a certain extend. So this algorithm adopted local area standard deviation to fuse the low-frequency coefficients. At first, get the local area standard deviation σ^{A} (x, y) and σ^{B} (x, y) of C^{A}_{j0} (x, y) and C^{B}_{j0} (x, y) according to Eq. 1, where the size of $N_1 \times M_1$ is 3×3 or 5×5. Then choose the coefficients by Eq. 2, where th is the test threshold:

$$\sigma = \sqrt{\frac{\sum_{i=-(N_1-1)/2}^{(N_1-1)/2}\sum_{j=-(M_1-1)/2}^{(M_1-1)/2}[C_{j0}(x+j,y+j)-\overline{C_{j0}}(x,y)]^2}{N_1 \times M_1}} \quad (1)$$

$$C^{F}_{j0}(x,y)=\begin{cases} C^{A}_{j0}(x,y) & \sigma^{A}-\sigma^{B}>th \\ C^{A}_{j0}(x,y)\times 0.5+C^{B}_{j0}(x,y)\times 0.5 & |\sigma^{A}-\sigma^{B}|\le th \\ C^{B}_{j0}(x,y) & \sigma^{A}-\sigma^{B}>th \end{cases} \quad (2)$$

At last, get the fused low-frequency coefficient C^{F}_{j0} (x, y).

High-frequency sub-band coefficient fusion: In order to better reserve the energy information of the image, the tower filter just adopted 1-layer decomposition. The directional decomposition level is 2. So the directional subband number of the whole high-frequency is $2^2 = 4$.

Beamlet edge detection: The Beamlet transform method is the integral of image function on the Beamlet basis. Suppose f (x_1, x_2) is the continuous function on each binary block. And the Beamlet transform of f (x_1, x_2) is defined as the line integral:

$$T_f(b) = \int_b f(x(l))dl, \quad b \in B_{n,\delta} \quad (3)$$

where, b is a Beamlet. $B_{n,\delta}$ is the Beamlet dictionary of the n×n image with the resolution δ. x (l) is the function of the x_1 and x_2 on the b-direction. T_f (B) is the beamlet transform coefficients.

This algorithm did edge detection on the 4 directional subband coefficient of the original images A and B to get the edge images E_{1A}, E_{2A}, E_{3A}, E_{4A}, E_{1B}, E_{2B}, E_{3B}, E_{4B}.

The marginal density function and its differences calculation: The image edge density is the ratio of the pixels number in the edge line to the total pixels number in this region in the edge image. For a image of size M×N, its edge density is:

$$\rho = \frac{\sum_{i=1}^{M-1}\sum_{j=0}^{N-1} p_{ij}}{M \times N} \quad (4)$$

where, ρ denotes the edge density of the image. M and N represent the row pixel and the column pixel, respectively. i and j identify the coordinates of the image pixels. p_{ij} indicates the value of the pixel (i, j). p_{ij} = 1 denotes the edge. p_{ij} = 0 denotes the background. According to the Eq. 4, the edge density feature of each pixel can be get as follow steps:

Step 1: A L*L area with the point (i, j) was chosen as center. The edge density was defined as the ratio of the pixels number in the edge to the total pixels number in the whole area:

$$\rho_{ij} = \frac{\sum_{i=1}^{L-1}\sum_{j=0}^{L-1} p_{ij}}{L^2} \quad (5)$$

where, ρ_{ij} denotes the edge density of the point (i, j). p_{ij} denotes the value the pixel (i, j). $p_{ij} = 1$ denotes the edge. $p_{ij} = 0$ denotes the background

Step 2: The directional subband component edge images of the two original images A and B was recorded as E_{1A}, E_{2A}, E_{3A}, E_{4A}, E_{1B}, E_{2B}, E_{3B}, E_{4B}. According to the Eq. 5, the edge densities of them were calculated. The results were recorded as DE_{1A}, DE_{2A}, DE_{3A}, DE_{4A}, DE_{1B}, DE_{2B}, DE_{4B}, DE_{1B}

Step 3: Finally, the differences of these edge densities are shown as follows:

$$sub_1 = DE_{1A}\text{-}DE_{1B}$$
$$sub_2 = DE_{2A}\text{-}DE_{2B}$$
$$sub_3 = DE_{3A}\text{-}DE_{3B}$$
$$sub_4 = DE_{4A}\text{-}DE_{4B}$$

The directional subband coefficients fusion: Fuzzy C-Means (FCM) is a popular clustering algorithm. Its iteration adopts hill-climbing algorithm to search optimal solution. This algorithm used FCM to do double threshold, respectively on sub_1, sub_2, sub_3 and sub_4. The results are the thresholds th_{11}, th_{12}, th_{21}, th_{22}, th_{31}, th_{32}, th_{41}, and th_{42}. The high-frequency sub-band coefficient fusion rules in four directions are shown as follows:

$$\begin{cases} sub_1 > th_{11} & C_{1F}(i,j) = C_{1A}(i,j) \\ th_{12} < sub_1 < th_{11} & C_{1F}(i,j)\ weightingfusion \\ sub_1 < th_{11} & C_{1F}(i,j) = C_{1B}(i,j) \end{cases} \quad (6)$$

$$\begin{cases} sub_2 > th_{21} & C_{2F}(i,j) = C_{2A}(i,j) \\ th_{22} < sub_2 < th_{21} & C_{2F}(i,j)\ weightingfusion \\ sub_2 < th_{21} & C_{2F}(i,j) = C_{2B}(i,j) \end{cases} \quad (7)$$

$$\begin{cases} sub_3 > th_{31} & C_{3F}(i,j) = C_{3A}(i,j) \\ th_{32} < sub_3 < th_{31} & C_{3F}(i,j)\ weightingfusion \\ sub_3 < th_{31} & C_{3F}(i,j) = C_{3B}(i,j) \end{cases} \quad (8)$$

$$\begin{cases} sub_4 > th_{41} & C_{4F}(i,j) = C_{4A}(i,j) \\ th_{42} < sub_4 < th_{41} & C_{4F}(i,j)\ weightingfusion \\ sub_4 < th_{41} & C_{4F}(i,j) = C_{4B}(i,j) \end{cases} \quad (9)$$

Then the local variance weighted fusion rule was used on the weighted fusion.

By the above fusion rules, the high-frequency coefficients C_{1A} (i, j), C_{1B} (i, j), C_{2A} (i, j), C_{2B} (i, j), C_{3A} (i, j), C_{3B} (i, j), C_{4A} (i, j) and C_{4B} (i, j), were fused. The fused high-frequency coefficients were C_{1F} (i, j), C_{2F} (i, j), C_{3F} (i, j) and C_{4F} (i, j).

Consistency correction: The last step was to do consistency correction on the fused sub-band coefficients. The 3×3 neighborhood of each pixel in fusion coefficient was scanned. Then the pixels numbers of the original image A and B were counted, respectively. And the numbers were compared. If the pixels number in one pixel 3×3 neighborhood from the original image A is larger than the number from the original image B, the value of this pixel in the fused image takes the value of this pixel in the original image A. Otherwise, the value takes the value of this pixel in the original image B.

By the above fusion, the fused low-frequency coefficient and four fused low-frequency coefficients were got. They are C^{F}_{j0} (x, y), C_{1F} (x, y), C_{2F} (x, y) and C_{4F} (x, y).

At last, the NSCT inverse transform was done on the fused coefficients to get the fused image.

EXPERIMENTAL RESULTS AND ANALYSIS

Experiment data: This study used two experiment sets to verify the fusion performance of this algorithm. The size of the experiment image was 256×256. The images of one experiment set are the positron emission scanning (PET) and the Magnetic Resonance Imaging (MRI). The images of one experiment set are the Computed Tomography (CT) and the MRI image. These images are all the visible human standard images used in the U.S. National Library of Medicine.

The experiment parameter setting: The comparison methods used in the experiment were the DWT method, Contourlet method and the NSCT method. The experimental platform is MATLAB 7.4. The computer clocked is 3.0 GHz and the computer memory is 2 GB. In the aspect of the parameter setting of the experiment, the DWT method adopted dB 4 wavelet filter. The direction decomposition series of the Contourlet method and the NSCT method are 2, 3, 3. In the Contourlet method, the scale decomposition filter was the "9-7" filter and the direction decomposition filter was the "pkva" filter. In the NSCT algorithm, the scale decomposition filter was "maxflat" filter and the direction decomposition filter was the "pkva" filter. The filter of this algorithm was same with the NSCT method but this algorithm used the scale 1-layer in the scale.

Evaluation criteria: This study evaluated the image in the aspect of entropy (EN), Mutual Information(MI), Average Gradient(AvG) and $Q^{AB/F}$ (Qu *et al*., 2002). EN indicates that the fused image contains the amount of information. MI shows the amount of information obtained from the original image. AvG expresses the ability that image expresses the minute details of contrast. It represents the image clarity. The larger of the $Q^{AB/F}$ value, the richer of the fused image edge information.

Experiment result analysis: Figure 3a is PET image shows the functional status of the organ corresponding position. Figure 3b is MRI image shows the soft tissue. Its brightness is correlated with the hydrogen atoms number in human tissue. Figure 3c-f are the results fused by various methods. The results show that the DTW method (Fig. 3c) lost most data and has low clarity. The Contourlet method (Fig. 3d) lost most MRI lines details on while of capturing functional areas in the corresponding position of certain organ. The NSCT method (Fig. 3e)

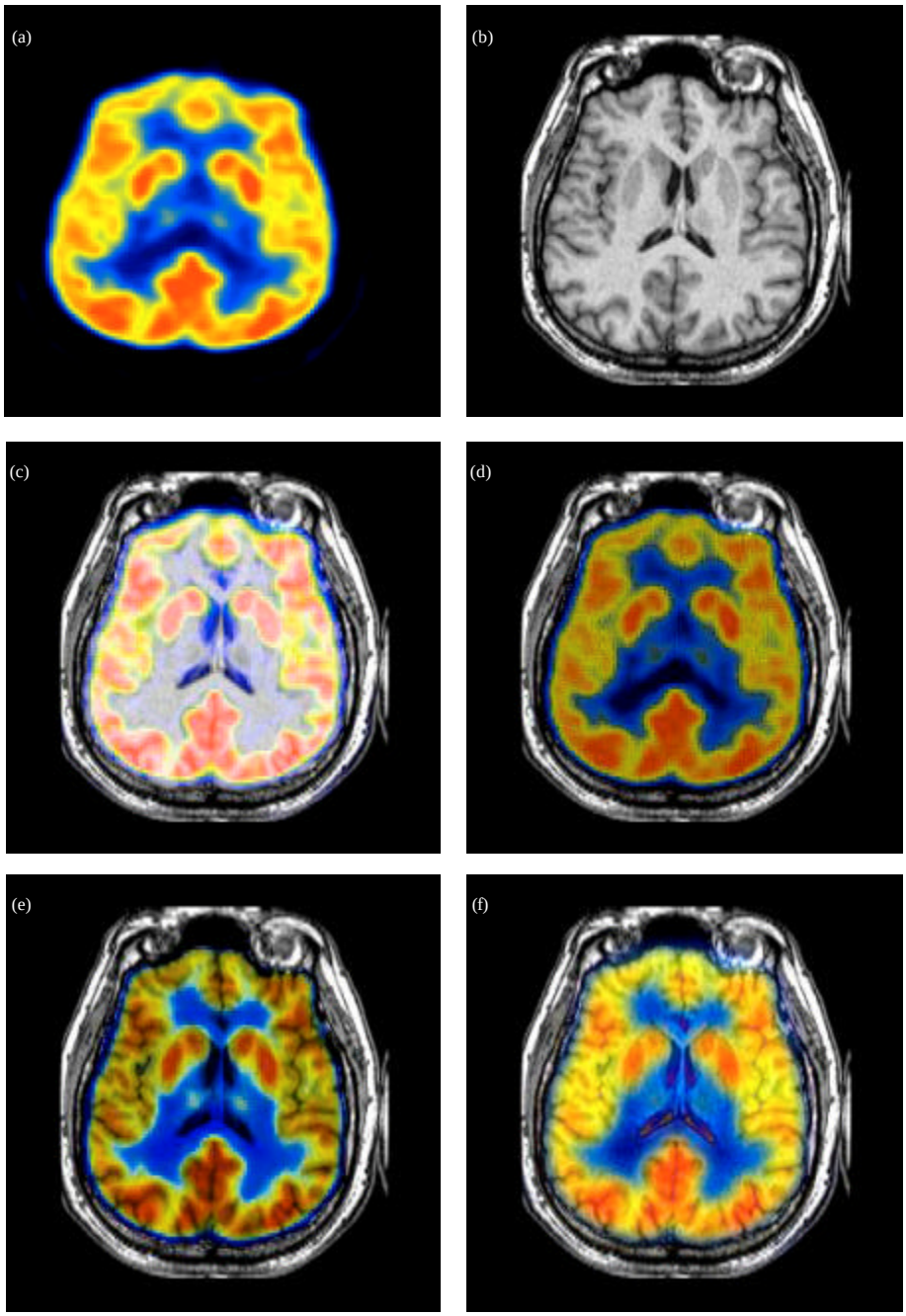

Fig. 3(a-f): Fusion results of PET and MRI images (a) Original PET image, (b) Original MRI image, (c) DWT method, (d) Contourlet method, (e) NSCT method and (f) Proposed method

has better effect than the Contourlet method because of its translational invariance. It can capture most lines and functional information. But the result is not so clear. The method in this study (Fig. 3f) adopted Beamlet transform to detect lines. So the lines in the soft tissue are very clear in the result. And this method can better reserve the functional area information. It has the best effect in the four methods.

Figure 4a is CT image shows the skeletal morphology of the human body. Its brightness is

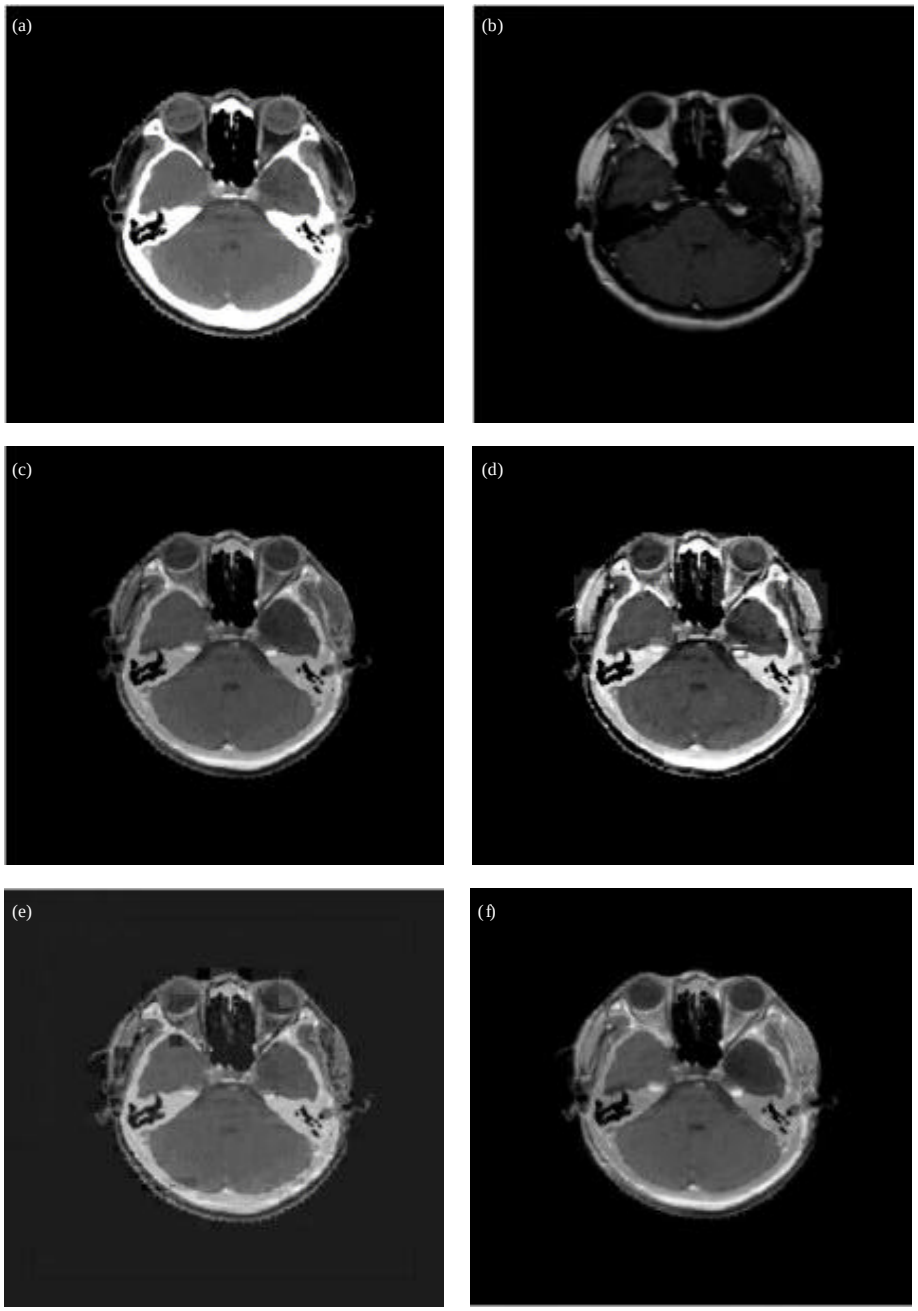

Fig. 4(a-f): Fusion results of CT and MRI images (a) Original CT image, (b) Original MRI image, (c) DWT method, (d) Contourlet method, (e) NSCT method and (f) Proposed method

Table 1: Quantitative comparison of the fusion results with different methods

Methods	Entropy	Mutual information	Average gradient	Edge retention
Discrete cosine transform	5.4587	3.5847	3.2578	0.4586
Contourlet	5.7859	3.4985	4.5225	0.5485
Non-subsampled contourlet transformation	5.8952	3.5946	4.7539	0.5823
Proposed method	6.0126	3.6124	6.2154	0.7214

correlated with the human tissue density. Figure 4b is MRI image which mainly shows the soft tissue. The fused results shows that the Contourlet method (Fig. 3d) and the NSCT method (Fig. 3e) could better reserve the edge information. But the singular points are not clear enough. The DCT method (Fig. 3c) can better reserve the singularity of the points. But the edge is not clear enough. The fused result of this algorithm can clearly show the singular points and the lines reserved in the edge of the tissue. It has the best effect in the four methods.

The quantitative comparisons of the fused results are shown in the Table 1. The values in this study are all higher than values of other methods.

Table 1 shows that this algorithm has the best results in the aspect of EN, MI, AvG and $Q^{AB/F}$ in the four methods. The reason is that this algorithm makes full use of the superiority of the Beamlet transform in the line detection. It makes the results has clear wire edge and details.

CONCLUSION

Based on the NSCT transform, this study proposed a novel medical image fusion method. Compared with the traditional Contourlet or NSCT method, this algorithm added the image linear features detected by the Beamlet transform to the image fusion process. The fused image with obvious linear edge detail characteristics can be observed. Compared with the traditional NSCT image, this algorithm made use of the superiority of the Beamlet transform in the image line detection to effectively extract the image edge information, pick up the linear feature from the image with strong noise and express the edge information detected by the Beamlet transform by the form of edge density. The experiment results and the quantization analysis shows that this algorithm can be better used in image fusion and has superiority compared with the wavelet or Contourlet multi-scale analysis methods.

ACKNOWLEDGMENTS

Project was supported by National Natural Science Foundation of China (60962004 and 61162016) and Lanzhou Jiaotong University Young Scholar Fund (2012003).

REFERENCES

Da Cunha, A.L., J. Zhou and M.N. Do, 2005. Nonsubsampled contourlet transform: Filter design and applications in denoising. Proceedings of the IEEE Conference on Image Processing, (IP'05), Genova, pp: 749-752.

David, L.D. and H. Xiaoming, 2001. Beamlets and multi-scale image analysis. Springer Press, Berlin, pp: 149-196.

Guanqun, T., L. Dapeng and L. Guanghua, 2004. Application of wavelet analysis in medical image fusion. J. Xidian Univ., 31: 51-60.

Kong, W.W., Y.J. Lei, Y. Lei and J.X. Hua, 2011. Fusion method for gray-scale visible light and infrared images based on improved NSCT. Control Decision, 25: 1607-1612.

Lei, W., L. Bin and T. Lianfang, 2011. Medical image fusion based on shift-invariant shearlet transformation. J. South China Univ. Technol., 39: 145-152.

Li, F., Z. Yudong, Z. Zhenyu, P.S. David, W. Shuihua and W. Lenan, 2010. An improved image fusion algorithm based on wavelet decomposition. J. Convergence Inform. Technol., 5: 15-21.

Ling, T., Q. Zhiyu and Q. Chunxiao, 2008. Fusion technology of medical image based on wavelet. Transform modulus maximum. J. South China Univ. Technol., 36: 69-74.

Qu, G., D. Zhang and P. Yan, 2002. Information measure for performance of image fusion. Elect. Lett., 38: 313-315.

Rahmim, A. and H. Zaidi, 2008. PET versus SPECT: Strengths, limitations and challenges. Nucl. Med. Commun., 29: 193-207.

Yang, L., B.L. Guo and W. Ni, 2008. Multimodality medical image fusion based on multiscale geometric analysis of contourlet transform. Neurocomputing, 72: 203-211.

Zhang, Q. and B. Guo, 2008. A remote sensing image fusion algorithm based on the non-subsampled Contourlet. J. Optics, 28: 74-80.

Zhang, Q. and B.L. Guo, 2007. Fusion of infrared and visible light images based on nonsubsampled Contourlet transform. J. Infrared Millimeter Waves, 26: 476-480.